Construction and Investigation of an lncRNA-miRNA-mRNA Regulatory Network of Pancreatic Cancer via bioinformatics analysis

zilin yang
Department of Gastroenterology, Ruijin Hospital afliated to Shanghai Jiao Tong University School of Medicine, Shanghai, China

yuming tang
Department of Gastroenterology, Ruijin Hospital afliated to Shanghai Jiao Tong University School of Medicine, Shanghai, China

xuejiao wu
Department of Gastroenterology, Ruijin Hospital afliated to Shanghai Jiao Tong University School of Medicine, Shanghai, China

jiancheng wang
Department of General Surgery, Ruijin Hospital afliated to Shanghai Jiaotong University School of Medicine, Shanghai, China

weiyan yao (ywy11419@rjh.com.cn)
Department of Gastroenterology, Ruijin Hospital afliated to Shanghai Jiao Tong University School of Medicine, Shanghai, China

Research Article

Keywords: pancreatic cancer, bioinformatics, ceRNA, microRNA-130b

Posted Date: March 14th, 2022

DOI: https://doi.org/10.21203/rs.3.rs-1433634/v1

Abstract

Purpose

Pancreatic cancer causes a malignant digestive tumour with an unfavourable prognosis and insidious onset. The regulation mechanisms of pancreatic cancer were connected to the abnormal accommodate of diverse signaling pathways. Studies had increasingly indicated that long non-coding RNAs (lncRNAs), microRNAs (miRNAs), and messenger RNA (mRNAs) could play crucial roles during tumorigenesis. This study designs to detect functional genes and determine the potential molecular mechanisms of pancreatic cancer through bioinformatics.

Methods

We made a comprehensive comparison on the RNA-sequencing using the Gene Expression Omnibus (GEO) and established a dysregulated lncRNA-miRNA-mRNA network. In addition, several functional analyses in the competing endogenous RNAs (ceRNA) network were conducted by Gene Ontology (GO), Kyoto Encyclopedia of Genes and Genomes (KEGG). In addition, survival analysis and clinical feature analysis were made by Gene Expression Profiling Interactive Analysis (GEPIA) and linkedOmics. Proliferation, migration tests were selected to examine the roles of mir-130b in pancreatic cancer.

Results

23 lncRNAs, 40 miRNAs and 1613 mRNAs were aberrantly expressed in pancreatic cancer. We constructed a dysregulated ceRNA network with 11 lncRNAs, 19 miRNAs, and 66 mRNAs. A group of 121 interconnections was constructed in the ceRNA network. These upregulated DEmRNAs were mainly enriched in the mitotic spindle, were involved the transcription by RNA polymerase II, were related to E-box binding and participated in bacterial invasion of epithelial cells and yersinia infection etc. in contrast, the these upregulated DEmiRNAs were mainly enriched in spanning component of the plasma membrane, were involved in pyrimidine nucleobase catabolic process, were related to pyridoxal phosphate binding and participated in beta-Alanine metabolism and propanoate metabolism etc.. The survival analysis showed that 1 lncRNAs, 4 miRNAs, and 18 mRNAs might be potential factors for the prognostic prediction of pancreatic cancer. The strong positive relationships were found between candidate lncRNAs and candidate mRNAs targeted by miR-130b, CYTOR interacts with FRMD6 and TCF4, while HOXA11-AS interacts with MET regulated by miR-130b. MiR-130b was found that its overexpression could inhibit the proliferation and migration of pancreatic cancer cells, and lower expression of miR-130b was connected with longer survival of pancreatic cancer patients.

Conclusion

Our research provided further acknowledges the molecular mechanisms underlying pancreatic cancer and laid strong ground for improving pancreatic cancer diagnosis and prognosis by establishing the lncRNA-miRNA-mRNA regulatory network via bioinformatics analysis.

Introduction

As one of the most quickly fatal cancers of worldwide scope, pancreatic cancer had increasing incidence and mortality over the past decade [1]. And its pitiful 5-year survival rate is below 9% in the advanced tumour

stage[2]. Pancreatic cancer is closely regulated by a multi-step course of genetic and epigenetic changes during its pathophysiology. Nevertheless, the inner molecular mechanisms are still ambiguous.

Previously, numerous microarrays and bioinformatics approaches have been performed to study the potential tumorigenesis mechanisms of cancer. For instance, bioinformatics has been used to find out the potential key genes and pathways in glioblastoma from GEO datasets [3]. In addition, a ferroptosis-related long non-coding RNA (lncRNA) signature and the tumor microenvironment, therapeutic response, and prognosis value in gastric cancer have been discovered previously via bioinformatics analysis [4]. A similar situation that a lncRNA-miRNA-mRNA network was conducted by combining of different kinds of RNAs expression profiles using bioinformatics analysis in gastric carcinoma [5]. In a word, it is necessary to further study the potential tumorigenesis mechanism of pancreatic cancer via integrated bioinformatics.

In our study, differentially expressed mRNAs (DEmRNA), differentially expressed miRNAs (DEmiRNAs) and differentially expressed lncRNAs (DElncRNAs) were screened out from the GEO database. GO and KEGG analyses of DEGs involved in the ceRNA network were also demonstrated. Furthermore, we analysed ceRNA network to explore each kind of molecular interaction. We performed some inhibiter or promoter factors that may be related to the biological mechanisms in pancreatic cancer. Finally, we explored the position of miR-130b in clinicopathological features of pancreatic cancer. The proposed lncRNA-miRNA-mRNA network may provide extra information on the molecular regulatory mechanism of pancreatic cancer.

Materials And Methods

1. Data collection and pre-processing

The compared different RNAs expression profiles between pancreatic cancer tissues and adjoining normal tissues got from the National Center of Biotechnology Information (NCBI) GEO dataset (https://www.ncbi.nlm.nih.gov/geo/). The already published reports were made to compare the RNAs expression profiles between pancreatic cancer (PC) tissue and noncancerous pancreatic (NC) tissue from patient. The raw miRNAs expression profiles were obtained from the GSE24279 (136 PC tissue and 22 NC tissue), GSE32678 (25 PC tissue and 7 NC tissue), and GSE41369 datasets (9 PC tissue and 9 NC tissue). GSE55643 (45 PC tissue and 8 NC tissue), GSE56560 28 PC tissue and 7 NC tissue) and GSE60979 (49 PC tissue and 12 NC tissue) are used as raw lncRNAs datasets. Another three datasets, including GSE56560 (28 PC tissue and 7 NC tissue), GSE60970 (49 PC tissue and 12 NC tissue), and GSE62165 (118 PC tissue and 13 NC tissue) were selected as raw mRNAs datasets.

2. Identification of differentially expressed genes

In this study, GEO2R (http://www.ncbi.nlm.nih.gov/geo/geo2r/) [6] was used to filter DElncRNAs, DEmRNAs and DEmiRNAs between tumour and non-tumor samples separately in each dataset. The differently expressed RNAs were met to the same cut-off value as $P<0.05$ and |log(Fold Change, FC)| >1.

3. Construction of ceRNA Network

Potential interactions between DEmiRNAs and DEmRNAs were found by using miRWalk2.0 (http://mirwalk.umm.uni-heidelberg.de/), which included both Target Scan[7] dataset and miRDB[8] dataset. A

score≥0.95 was used as the cutoff value in the prediction interaction analysis using miRWalk. Only those recognized by these criteria could be regarded as candidate DEmiRNAs-DEmRNAs pairs for further analysis. The interaction between candidate DEmiRNAs and DElncRNAs were predicted by LncBase v2.0 [9] (www.microrna.gr/LncBase) with a score≥0.4. Visualizing the regulatory RNAs interact coadjustment networks were made by Cytoscape software (version 3.6.1). The whole human genome was restricted to be set as a background, and results were evaluated for significance with $P<0.05$.

4. Gene ontology and KEGG pathway enrichment analysis

The Enrichr (https://maayanlab.cloud/Enrichr/) was used to reveal GO and KEGG analysis on significant DEGs and target genes of DEmiRNAs[10]. The species was restricted to Homo sapiens. GO terms were set up with three parts: molecular function (MF), cellular component (CC), and biological process (BP).

5. Co-expression regression analysis between DElncRNAs and DEmRNAs

The GSE60979 datasets were adopted for co-expression regression analysis which set by statistical software SPSS 26.0 between DElncRNAs and DEmRNAs.

6. Validation of DElncRNAs and DEmRNAs

To validate the DElncRNAs and DEmRNAs, We get the expression profile between PC tissues and NC tissues by using Gene Expression Profiling Interactive Analysis (GEPIA, http://gepia.cancer-pku.cn/detail.php) [11]. It included data from The Cancer Genome Atlas (TCGA, https://cancergenome.nih.gov/)[12] and the Genotype-Tissue Expression (GTEx, http://commonfund.nih.gov/GTEx/)[13].

7. Clinical feature analysis of ceRNA network

The expression of hub lncRNA and mRNA in TCGA and GTEx datasets was caught to make our analysis more reliable by GEPIA and verified the hub miRNA expression in TCGA datasets by linkedOmics (http://www.linkedomics.org/login.php)[14]. It was regard genes as statistically significant when met to $|\log_2 FC| > 1$ and p-value < 0.05.

8. RNA extraction and real-time quantitative PCR (RT-qPCR)

We selected 11 pancreatic cancer samples and pair no-tumourous samples from the Department of Gastroenterology of the Ruijin Hospital of Shanghai Jiao Tong University. Total tissue RNA was extracted by TRIzol Reagent (Invitrogen, Carlsbad, CA). TaqMan miRNA probes (Applied Biosystems, Foster City, CA) were utilized on detecting miR-130b expression according to the manufacturer's protocol and qualified by LightCycler® 480 II Real-Time PCR System software. snRNA was regarded as an internal reference to normalize the data, and there were 3 replicates per sample. Pancreatic cancer patients involved in our research got official approval from the Ruijin Hospital ethics committee.

9. Cell lines

ASPC-1 cell and MIA PaCa-2 cell were pancreatic cancer cell lines and were purchased from Shanghai Institute of Cell Biology (Shanghai, China). Both ASPC-1 cells and MIA PaCa-2 cells were incubated at 37 °C, and humidified 5% CO2, and were grown in DMEM (Gibco; Life Technologies, Carlsbad, CA, USA) joined with 10% FBS.

10. Cell transfection

After approximately 20 h of growth, PC cells seeded on plates were transfected using Lipofectamine 2000 (Invitrogen). Cells were set into three groups: transfection with miR-130b mimic and control mimic. For genetic manipulation, cells set on 6-well plates were transfected with miR-130b mimic at a totally of 100 pmol to get its expression rising. After treating 48h later, the cells were gathered for further experiments.

11. Cell proliferation assay

After 6 h of transfection, PC cells were cultured to 6-well plates were counted using a Celigo® Image Cytometer (Nexcelom, USA) and then seeded into 96-well plates at 6000 cells/well. After 24 hours, add 10 μl of CCK-8 reagent (Dojindo, Tokyo Japan) to each well of a 96-well plate and allow it to react for 2 hours. After incubation, measure the absorbance at 450 nm (OD value). The CCK8 assays were performed every 24 h for 96 h. All experiments were performed independently five times. During data analysis, the average value of each well at each time point was recorded, normalized by the value at the 0th hour, and then analyzed.

12. Cell wound-healing assay

PC ells were inoculated in 6-well plates and cultivated in DMEM with 2% FBS to inhibit the growth of wound-healing assay. After cells were grown to 70-90%, create scratches were made on the cell monolayer with a sterile 200μL aseptic pipette tip. At the time points of 0h, 24h, 48h and 72h after transfection, the linear wound was observed and photographed by a microscope (Olympus, Japan). The wound-healing result was statistically evaluated by ImageJ software.

13. Cell migration assays

PC cell migration capacity was defined in Transwell Permeable Supports (6.5 mm Insert; Costar, Cambridge, Mass). After one day of effective transfection, ASPC-1 or MIA PaCa-2 cells were suspended in FBS-free DMEM at 5*104 cells/mL and seeded the upper chamber at 5*103 cells per well. Fill the nether well with cell supernatant, 500 μl of DMEM with 20% FBS, to create a serum concentration gradient and then place at 37 ℃ and 5% CO2. After incubating for 24h, the cells were transferred through the filter. Fixed the cells with 4% polyformaldehyde for 20 min and subsequently rinsed with PBS several times, which both at room temperature. Cells were stained with 0.1% crystal violet for 20 min. Cotton swabs were used to softly wipe out residual cells left on the lower chamber lid. Follow the above steps to acquire images using Image-Pro Plus (IPP) 6.0. For each group, three separate cells were set to assess cell metastability.

Result

Identification of DElncRNAs, DEmiRNAs and DEmRNAs in pancreatic cancer

Microarray expression data of pancreatic cancer associated lncRNAs, miRNAs, and mRNAs were collected from GEO: This consisted of a total of 3 lncRNA expression datasets, including 122 pancreatic tumor tissue and 27 adjacent non-tumor tissue, 3 miRNA expression datasets, including 170 pancreatic tumor tissue and 38 non-tumor tissue, and 3 mRNA expression datasets, including 195 pancreatic tumor tissue and 32 non-tumor tissues (Table 1).

Table 1. Selected GEO dataset

Microarray	GEO accession	Number of tumour samples	Number of adjacent non-tumor samples
LncRNA microarray	GSE55643	45	8
	GSE56560	28	7
	GSE60979	49	12
	Total	122	27
miRNA microarray	GSE24279	136	22
	GSE32678	25	7
	GSE41369	9	9
	Total	170	38
mRNA microarray	GSE56560	28	7
	GSE60979	49	12
	GSE62165	118	13
	Total	195	32

Using thresholds of $|Log_2FC|>1$ in at least two datasets and p-value<0.05 in three datasets, the results show that 23 DElncRNAs (Table S1), including 15 upregulated DElncRNAs and 8 downregulated DElncRNAs, 40 DEmiRNAs(Table S2), including 31 upregulated DEmiRNAs and 9 downregulated DEmiRNAs, 1613 DEmRNAs (Table S3), including 1069 upregulated DEmRNAs and 544 downregulated DEmRNAs, were significantly abnormal expressed in pancreatic cancer. The top 5 obvious upregulated and downregulated DElncRNAs, DEmiRNAs and DEmRNAs were respectively shown in Table 2, 3, 4.

Table 2. Top 5 significantly up-regulated and top 5 downregulated DEmiRNAs in three GEO dataset.

		Pancreatic cancer (*n* = 170), normal pancreas (*n* = 38)					
miRNA name	Up	GSE24279		GSE32678		GSE41369	
	/Down	P value	Log2FC	P value	Log2FC	P value	Log2FC
hsa-miR-217	Down	3.56E-17	-5.42539			0.00152	-3.57232
hsa-miR-216a	Down	2.99E-11	-4.74284			0.000781	-2.63622
hsa-miR-130b	Down	5.91E-21	-3.91727			0.000984	-2.61235
hsa-miR-141	Down	0.0000481	-2.35824	0.002175	2.114211	0.0481	-2.12812
hsa-miR-200c	Down	5.16E-09	-1.85622	0.001694	2.216186	0.0499	-1.68123
hsa-miR-145	Up	6.82E-12	1.748881			7.79E-06	3.244704
hsa-miR-150	Up	8.67E-15	3.328354			0.000944	3.28386
hsa-miR-1825	Up	0.025	4.068449	0.010976	1.225039		
hsa-miR-135b	Up			2.14E-05	3.442542	4.63E-08	2.819987
hsa-miR-21	Up			8.13E-05	3.418418	0.000019	2.992536

Table 3.Top 5 significantly upregulated and downregulated DEmRNAs in three GEO dataset (logFC>3)

		Pancreatic cancer (*n* =195), normal pancreas (*n* =32)					
mRNA name	Up/	GSE56560		GSE60980		GSE62165	
	down	P value	Log2FC	P value	Log2FC	P value	Log2FC
ALB	down	6.2E-09	-5.929303	0.000022	-4.49572445	1.08E-14	-5.3
PNLIPRP1	down	0.000208	-4.93908	0.00312	-3.19119699	1.53E-15	-6.15
SERPINI2	down	0.00000774	-4.562986	0.000383	-4.02319809	1.94E-11	-6.47
CELA2A	down	0.00123	-4.271562	0.0086	-3.82716481	0.000000262	-6.02
AQP8	down	0.000000552	-3.68139	0.00000159	-4.06761851	9.79E-15	-6.17
MMP11	up	0.0000763	1.952182	2.59E-11	3.88137784	2.29E-27	4.86
GPRC5A	up	1.01E-12	3.512951	8.64E-10	2.2962543	3.55E-26	4.32
SLC6A14	up	0.00000065	3.930053	0.00000325	2.99596191	2.08E-14	4.65
POSTN	up	5.24E-09	4.378546	0.00000458	3.02612901		
CEACAM6	up	1.26E-11	4.549112	5.42E-08	3.9202177	4.25E-13	3.96

Table 4.Top 5 significantly upregulated and downregulated DElncRNAs in three GEO dataset.

		Pancreatic cancer (*n* = 122), normal pancreas (*n* =27)					
LncRNA name	Up/ down	GSE55643		GSE60980		GSE56560	
		P value	Log2FC	P value	Log2FC	P value	Log2FC
LINC00671	Down			4.35E-06	-1.20411	3.02E-15	-2.15519
LINC00029	Down			2E-07	-1.73827	5.79E-07	-1.03315
FAM167A-AS1	Down			0.000514	-1.37194	1.43E-10	-1.25994
LINC00339	Down	0.00262	-1.50678	5.93E-06	-1.55368	1.15E-08	-1.88799
AKR7A2P1	Down	8.94E-05	-1.30069	4.25E-05	-1.87539		
KRT19P2	Up	0.0285	1.279934	2.06E-09	2.987603		
KRT16P6	Up	0.00594	2.026907	2.95E-07	2.754911		
KRT16P2	Up	0.000937	2.834359	3.51E-08	3.462639		
AFAP1-AS1	Up	0.000946	3.660372	0.000138	1.438305	0.0103	1.495363
HOXA11-AS	Up	0.00086	3.700575	0.000532	1.507758		

Prediction of DEmiRNA-targeted DEmRNAs by miRWalk

We used the miRwalk database to predict the target gene on the above 40 DEmiRNA. A total of 2600 miRNA-mRNA relationship pairs were contained 34 DEmiRNAs and 1798 target mRNAs. By intersecting with DEmRNAs, a total of 83 miRNA-mRNA relationship pairs, including 23 DEmiRNAs and 69 DEmRNAs (Table S4), that 19 over-expressed DEmiRNAs downregulated 34 DEmRNAs (Figure 1A), while 4 under-expressed DEmiRNAs upregulated 35 DEmRNAs (Figure 1C).

Prediction of DElncRNA-DEmiRNA coaction by LncBase 2.0

We mapped the above mentioned 40 DEmiRNAs into the LncBase2.0 and searched for the DEmiRNA-targeted lncRNAs. By intersecting with DElncRNAs, There were 71 interactions between 32 DEmiRNAs (hsa-let-7d, hsa-let-7i, hsa-10a, hsa-125a-5p, hsa-125b, hsa-130b) and 12 DElncRNAs(RUNX1-IT1, HOXA11-AS, UNC5B-AS1, FAM167A-AS1, LINC01869, LINC00339, LINC00671, CMAHP, LINC00029, AFAP1-AS1, CYTOR, MIR4697HG). In detail, 7 over-expressed DElncRNAs downregulated 8 DEmiRNAs, while 5 under-expressed DElncRNAs upregulated 24 DEmiRNAs (Figure 2, Table S5).

Construction of ceRNA interaction network

We established a ceRNA regulatory network with pre-treated data (Figure 3, Table S6). In the network, there are 11 DElncRNAs, 19 DEmiRNAs, and 66 DEmRNAs. At length, 5 under-expressed DElncRNA upregulate 15 DEmiRNAs, while 15 over-expressed DEmiRNAs downregulate 31 DEmRNAs; 6 over-expressed DElncRNAs downregulate 4 DEmiRNAs, while 4 down-expressed DEmiRNAs over-regulate 35 DEmRNAs.

Furthermore, we topologically calculated the connectivity among each gene to elucidate its significance in the ceRNA interaction network (Table 5, Table S7). They were considered to be the pivotal genes with degree>5

among the lncRNAs and miRNAs, including LINC00029, FAM167A-AS1 , LINC00671; hsa-miR-130b; hsa-miR-141; hsa-miR-200c; hsa-miR-23a; hsa-miR-217; hsa-miR-125a-5p; hsa-miR-24; hsa-miR-27a; hsa-miR-199a-5p; hsa-miR-34a; hsa-miR-34c-5p. Since hsa-miR-130b was the most connected degree with 20 in the ceRNA regulatory network, we inferred that it might have a strong impact on the pancreatic cancer process. The lncRNA-miRNA-mRNA network also revealed that DElncRNAs indirectly acted with DEmRNAs.

Table 5. Topology parameters of 14 hub gene (degree>5) in the ceRNA network

Gene	Type	Betweenness	Closeness	Degree
LINC00029	lncRNA	678.87489	26.48333	10
FAM167A-AS1	lncRNA	782.85275	25.5	9
LINC00671	lncRNA	641.19704	25.9	8
hsa-miR-130b	miRNA	1261.33333	27.31667	20
hsa-miR-141	miRNA	784.66667	20.91667	10
hsa-miR-200c	miRNA	635.66667	19.45	10
hsa-miR-23a	miRNA	528.35005	24.23333	9
hsa-miR-217	miRNA	576.33333	19.45	8
hsa-miR-125a-5p	miRNA	426.70879	21.85238	7
hsa-miR-24	miRNA	486.77879	22.51667	7
hsa-miR-27a	miRNA	371.21975	22.9	7
hsa-miR-199a-5p	miRNA	528.86061	21.05	6
hsa-miR-34a	miRNA	227.63663	22.23333	6
hsa-miR-34c-5p	miRNA	175.35741	22.23333	6

Function enrichment analysis of DEmRNAs in ceRNA network

Using the Enrichr, we analyze the GO and KEGG analysis of 66 DEmRNAs based on the constructed ceRNA interaction network.

Significantly, GO BP analysis performed that candidate genes targeted by downregulated DEmiRNAs were participated in positive regulation of transcription by RNA polymerase II, positive regulation of transcription, DNA-templated (Figure 4A). CC analysis performed that these candidate genes were significantly concentrated in mitotic spindle, cell-cell junction and adherens junction (Figure 4C). For MF items, they took part in E-box binding, disordered domain specific binding and phosphatidylinositol-3,4,5-trisphosphate binding (Figure 4E). While for GO BP analysis demonstrated that candidate genes targeted by upregulated DE-miRNAs were significantly involved in the pyrimidine nucleobase catabolic process, pyrimidine nucleobase metabolic process and regulation of cytokine production (Figure 4B). CC analysis performed that these genes were significantly enriched inspanning components of the plasma membrane, PRC1 complex and endoplasmic reticulum membrane (Figure

4D). At last, MF analysis for these genes showed that they were major enriched in pyridoxal phosphate binding, potassium ion transmembrane transporter activity, and prostaglandin E receptor activity (Figure 4F).

Further, KEGG pathway analysis was revealed for 66 DEmRNAs based on the constructed ceRNA network. Candidate genes targeted by downregulated DEmiRNAs were significantly taking participated in bacterial invasion of epithelial cells, yersinia infection, microRNAs in cancer, transcriptional misregulation in cancer, adherens junction, melanoma, non-small cell lung cancer, Endocytosis, small cell lung cancer and prostate cancer (Table 6). The KEGG pathways for candidate genes targeted by upregulated DE-miRNAs were shown in Table 7.

Table 6. The top 10 enriched KEGG pathways for the intersection of target genes of downregulated DE-miRNAs and upregulated DEGs.

Term	count	Gene	p-value
Bacterial invasion of epithelial cells	3	CLTC;FN1;MET	3.29E-04
Yersinia infection	3	TBK1;WIPF1;FN1	0.001753
MicroRNAs in cancer	4	BMPR2;ZEB1;E2F3;MET	0.00203
Transcriptional misregulation in cancer	3	ZEB1;PPARG;MET	0.004548
Adherens junction	2	LMO7;MET	0.006854
Melanoma	2	E2F3;MET	0.007042
Non-small cell lung cancer	2	E2F3;MET	0.007042
Endocytosis	3	WIPF1;CLTC;ARAP2	0.00961
Small cell lung cancer	2	FN1;E2F3	0.011284
Prostate cancer	2	ZEB1;E2F3	0.012483

Table 7. The top 10 enriched KEGG pathways for the intersection of target genes of upregulated DE-miRNAs and downregulated DEGs

Term	count	Gene	p-value
beta-Alanine metabolism	2	ALDH6A1;ABAT	9.84E-04
Propanoate metabolism	2	ALDH6A1;ABAT	0.001265
Valine, leucine and isoleucine degradation	2	ALDH6A1;ABAT	0.002509
Phosphonate and phosphinate metabolism	1	PCYT1B	0.009265
Selenocompound metabolism	1	CTH	0.026036
Mannose type O-glycan biosynthesis	1	B3GALNT2	0.035067
Proximal tubule bicarbonate reclamation	1	SLC4A4	0.035067
Renin-angiotensin system	1	ANPEP	0.035067
Maturity onset diabetes of the young	1	NR5A2	0.039553
Butanoate metabolism	1	ABAT	0.042532

Validation of DElncRNA and DEmRNAs in the ceRNA Network

TCGA and GTEx datasets were analyzed by using GEPIA to demonstrate that aberrant expression of DElncRNAs and DEmRNAs were significantly over-expressed between pancreatic cancer and normal pancreas tissues (Figure 5) based on optimal cutoff ($|Log_2FC| >1$, $p<0.01$).

For further research of the ceRNAs, we analyzed the association of the ceRNA network with clinical features in the TCGA database, such as neoplasm histologic grade and pathologic stage. The results showed that 1 lncRNA was associated with the pathologic stage, 2 miRNA were associated with years of birth, 4 miRNAs were associated with radiation therapy samples, 6 miRNAs were associated with pathologic M stage, and 18 mRNAs were connected to the clinical pathologic stage ($P < 0.05$; Figure 6-7, Table S8).

Relationship between key genes and overall survival

We conducted a survival analysis on each DElncRNA, DEmiRNA and DEmRNA in the ceRNA network to discover the potential prognosis RNA biomarker in pancreatic cancer. 1 DElncRNAs, 3 DEmiRNAs, and 19 DEmRNAs were tightly connected with overall survival, which met the cutoffs value (Figure 8, Table S9). Of these, 5 DEmRNAs appeared to exhibit protective functions, as pancreatic cancer patients with the higher expression level of these mRNAs were likely to get a longer prognosis. On the contrary, the remaining 1 DElncRNAs and 12 DEmRNAs were considered as risky factors because their expression was inversely connected to the prognosis of pancreatic cancer patients.

Positive correlation among the expression levels in ceRNA network

According to ceRNA theory, lncRNAs can positively influence mRNAs by competing with miRNAs for their binding sites. So we conducted a regression analysis between DElncRNAs and DEmRNAs targeted by miR-130b (Table S10), which was the most connected gene in the ceRNA network with a connection of degree 20. Intense positive associations were found between DElncRNAs and DEmRNAs, which were targeted by miR-130b in GSE60980 with an interaction score>0.4. It revealed the first three correlation coefficients of the interactions under the

regulation of miR-130b, in which CYTOR interacted with FRMD6 and TCF4, while HOXA11-AS interacted with MET(Figure 9).

Clinicopathologic Significance of miR-130b in Pancreatic Cancer Patients

miR-130b was tested by qRT-PCR in the 11 pairs of PC tissues and matched NC tissues. Compared to the matched noncancerous pancreatic tissues, 11 PC tissues showed lower miR-130b expression with the median fold change of 1.23 ($P<0.05$). Moreover, Kaplan–Meier curves revealed that increased miR-130b was connective with tightly longer survival time in pancreatic cancer patients ($p = 0.014$) (Figure 10B).

MiR-130b Inhibited Cell Proliferation in vitro

To assess the function of miR-130b on PC cell proliferation activity, the proliferation rate of miR-130b overexpressing cells was assessed every 24h for 72h. miR-130b was successfully overexpressed in ASPC-1 cells and MIA PaCa-2 cells. In general, miR-130b enhanced the proliferative capacity of PC cells, as shown by the serial measurements of proliferation rates (Figure 11). These results proved that miR-130b could inhibit pancreatic cancer cell proliferation.

MiR-130b Suppressed Migration of Pancreatic Cancer Cell

To discover how miR-130b affected on pancreatic cancer cells, we treated MIA PaCa-2 and ASPC-1 cells with miR-130b mimics and control mimics in 50 nM. With overexpression of miR-130b, the proliferation of MIA PaCa-2 and ASPC-1 cells were significantly suppressed by 32.60401% and 23.79411%, respectively ($P<0.01$, Figure 12).

In addition, we used transwell to analyse the function of miR-130b in the pancreatic cancer cell migration. We discovered that the count of migrating ASPC-1 cells with miR-130b overexpression (2285 cells/high power magnification field (HP)) was significantly less than matched control groups(3615 cells/HP; Figure. 13A). Similar results were also found in MIA PaCa-2 cells (Figure 13B). It further revealed that the miR-130b mediated the migration of pancreatic cancer cells.

Disscusion

To our knowledge, there were few reliable RNAs associated with pancreatic cancer, such as lncRNAs, miRNAs and mRNAs, which might be considered as special molecular biofactors for detection and risk stratification of pancreatic cancer. In this context, the expression data of lncRNAs, mRNA, and miRNA for 410 PC tissues and 78 controls were obtained from 7 GEO datasets. Based on the comprehensive integration of the RNAs expression data in our study, a ceRNA network was established to define the molecular interaction mechanism of ceRNA. Despite the extremely complex biogenesis profile of pancreatic cancer, DEGs can largely represent accomplice tumorigenesis as well as malignant metastasis. As a result, we took advantage of DEGs to build the lncRNA-miRNA-mRNA interaction network. In this study, we found out 23 DElncRNAs and 12 DElncRNAs targeted by DEmiRNAs in the in PC tissues compared with the control samples in this ceRNA network. One of them had a clear correlation with overall survival. Compared with the NC tissues, there were 40 upregulated DEmiRNAs in the PC tissues and 32 candidate DEmiRNAs as a target factor of DElncRNAs in the ceRNA regulatory network. Among them, 3 DEmiRNAs showed an obvious positive correlation with cancer overall survival. We also detected

1615 DEmRNAs in the PC tissues compared with the matched control group, of which 66 DEmRNAs targeted by DEmiRNAs were included in the ceRNA network. Among them, 23 DEmiRNAs were significantly associated with overall survival. The genes strongly connected with overall survival may manifest a future prognosis for pancreatic cancer.

In addition, we analyzed the functions and pathways of DEmRNAs participating in the ceRNA network using the Enrichr dataset. These upregulated DEmRNAs mediated by downregulated DEmiRNAs were mainly enriched in the mitotic spindle, were involved the transcription by RNA polymerase II, were related to E-box binding and participated in bacterial invasion of epithelial cells and yersinia infection etc. in contrast, the these upregulated DEmiRNAs were mainly enriched in spanning component of the plasma membrane, were involved in pyrimidine nucleobase catabolic process, were related to pyridoxal phosphate binding and participated in beta-Alanine metabolism and propanoate metabolism etc., which were greatly participant with carcinogenesis.

In this ceRNA regulation network, miR-130b was the most relevant RNAs with the majority DElncRNAs and DEmRNAs with connection degree 20. It suggested that miR-130b play a crucial role in the onset progress and prognosis of pancreatic cancer. In our research, we verified miR-130b could suppress cells to malignant proliferate and migrate in pancreatic cancer. Based on the previous studies, miR-130b is located in human chromosome 22, and lots of studies detected that miR-130b greatly influenced many kinds of cancers with low expressions, such as medulloblastoma (MB) [15], prostate cancer [16], and Multiple myeloma (MM)[17] etc. yet it was overexpressed in hepatocellular carcinoma (HCC) [18], oral squamous cell carcinoma (OSCC)[19], esophageal squamous cell carcinoma (ESCC) [20] etc. miR-130b was detected to low expression in MB samples compared with surrounding non-cancerous samples and it inhibited MB oncogenesis by mediate serine/threonine-protein kinase 1 (SIK1) [15]. Mu HQ etc. verified a feedback loop of miR-130b/TNF-α/NF-κB/VEGFA, which was strongly associated with angiogenic growth in prostate cancer, and miR-130b could be served as prospective remedial management for anti-giogenesis therapy [16]. What is more, the miR-130b suppressor could hold up glioma cells proliferation and invasion via the PTEN/AKT pathway and may be considered as a significant therapeutic measure for glioma [21]. On the contrary, miR-130b was significantly over-expressed in human HCC [18] and ESCC [20]. In our study, miR-130b was under-regulated in pancreatic cancer tissues, and the survival analysis of the present study revealed that pancreatic cancer patients with lower expression of miR-130b were likely to have a longer survival time. Thus, we suspected miR-130b could be an effective biomarker to forecast the further treatment effect and tumor progression of patients with pancreatic cancer.

Malignant insidious proliferation and metastasis were the primary reasons for unsatisfied prognosis in pancreatic cancer patients. Lots of studies have indicated that miRNAs played essential roles in metastasis and malignant proliferation of pancreatic cancer [22, 23]. This study showed miR-130b was obviously decreased in the pancreatic cancer samples. Moreover, patients with miR-130b overexpression got a longer survival time. We further confirmed the effective bio-function of miR-130b in pancreatic cancer cell migration. After overexpressing with miR-130b, the migration ability of MIA PaCa-2 and ASPC-1 cells was decreased. It greatly revealed that miR-130b could intensively participate in the pancreatic cancer malignant metastasis. Therefore, management to import miR-130b into cancer cells could be potentially viable for clinical treatment of pancreatic cancer, in especial for those with miR-130b under-expression.

Besides, we conducted an interaction analysis between DElncRNAs and DEmRNAs mediated by miR-130b. It revealed strong associations among some DElncRNAs and DEmRNAs regulated by miR-130b. Among them, CYTOR has the best correlation with FRMD6 ($P < 0.001$).

LncRNA CYTOR (also known as LINC00152) is located in human chromosome 2p11.2, and it was verified to be an oncogenic factor in the tumorigenesis process [24, 25]. It was found to be upregulated in many different cancer tissues [26, 27]. In nasopharyngeal carcinoma (NPC) tissues, a lower expression of CYTOR was positively associated with early tumor, clinical stages and poor prognosis. The study revealed that CYTOR could facilitate cell invasion and metastasis in NPC by competitive binding miR-613 to influence the expression of ANXA2 [28]. Similarly, in laryngeal squamous cell cancer (LSCC), a higher CYTOR expression was closely associated with LSCC patients with lymphatic metastasis or an early clinical stage, and CYTOR exerted an oncogenic effect on the tumorigenesis [29]. Mechanistically, a study reported that CYTOR could directly interact with miR-195 and increase its targets genes, and it may be used as a promising molecular target for NSCLC treatment strategy [30]. Another research revealed that CYTOR could develop drug resistance to oxaliplatin-induced apoptosis and promoted cancer EMT and metastasis by acting with β-catenin. The inner positive feed-forward loop between CYTOR and β-catenin might be a viable therapeutic target in the anti-metastatic strategy of colon cancer [31]. In the present study, CYTOR was strongly correlated with FRMD6 and TCF4. Furthermore, CYTOR and FRMD6 or TCF4 were all overexpressed in pancreatic cancer in datasets. The opposite interaction among miR-130b and CYTOR/FRMD6 or CYTOR/TCF4 in PC and NC tissues was further substantiated the decreasing miR-130b expression was on account of higher expression of CYTOR. Based on this study, it demonstrated that CYTOR could regulate FRMD6 or TCF4 expression to inhibit cell growth and invasiveness by competing with miR-130b to mediate the tumorigenesis process of pancreatic cancer.

In our study, LncRNA HOXA11-AS also got a high relationship with MET mediated by miR-130b. HOXA11-AS was a long non-coding RNA coded by HOXA11 antisense gene, which was situated on human chromosome 7p15.2. It played an important role in the occurrence and progression of multiple disease. For a instance, lncRNA HOXA11-AS functioned as an oncogene in malignancies including prostate cancer[32], NSCLC[33], oral cancer[34] and et al. HOXA11-AS could act as a tumor promote factor via regulating miRA-125a-5p/TMPRSS4 axis in breast cancer[35]. In gastric cancer, HOXA11-AS could activate ITGB3 in binding with miR-124-3p MRE sites and functioned as a promoter to acelebrate the cancer migration and invation[36]. In addition, HOXA11-AS was detected to aggravate microglia-induced neuroinflammation after traumatic brain injury[37]. In our study, we verified the relationship among HOXA11-AS-miR-130b-MET which also could be a potential axis in pancreatic cancer worth further studying.

Conclusion

In conclusion, we analyzed 23 DElncRNAs, 40 DEmiRNAs and 1613 DEmRNAs from 7 GEO datasets by bioinformatics. Additionally, we established an lncRNA-miRNA-mRNA interaction network in pancreatic cancer aiming to get a deeper cognition of the underlying molecular mechanism. The passways mediated by miR-130b, such as CYTOR/miR-130b/FRMD6, CYTOR/miR-130b/TCF4, and HOXA11-AS/miR-130b/MET, might be effective useful novel alternative diagnostic biomarkers or act as potential therapeutic targets in pancreatic cancer.

Abbreviations

lncRNA: long non-coding RNAs:

miRNA: microRNAs

mRNA: messenger RNA

GEO: Gene Expression Omnibus

ceRNA: competing endogenous RNAs

GO: Gene Ontology

KEGG: Kyoto Encyclopedia of Genes and Genomes

DEmRNA: differentially expressed mRNA

DEmiRNA: differentially expressed miRNA

DElncRNA: differentially expressed lncRNA

NCBI: National Center of Biotechnology Information

PC: pancreatic cancer

NC: noncancerous pancreatic

FC: Fold Change

RT-qPCR:real-time quantitative PCR

MF: molecular function

CC: cellular component

BP: biological process

GEPIA: Gene Expression Profiling Interactive Analysis

TCGA: The Cancer Genome Atlas

GTEx: the Genotype-Tissue Expression

HP: high power magnification field

MB: medulloblastoma

MM: Multiple myeloma

HCC: hepatocellular carcinoma

OSCC: oral squamous cell carcinoma

ESCC: esophageal squamous cell carcinoma

SIK1: serine/threonine-protein kinase 1

Declarations

Acknowledgements

We thank Dr. Yao for useful suggestions, Dr. Wang for collecting the samples, and Dr. Wu for efective direction during writing.

Authors' contributions

YZ, TY, and WX contributed to the information collection and related cell experiments. These three authors contributed equally to this work. WX and ZYP contributed to the statistical analysis process. YW and YZ contributed to experimental design. All authors read and approved the fnal manuscript.

Funding

Not applicable.

Availability of data and materials

The datasets analysed in this study can be found in the Gene Expression Omnibus (GEO) repository (https://www.ncbi.nlm.nih.gov/gds/) and The Cancer Genome Atlas (https://www.ncbi.nlm.nih.gov/gds/).

Ethics approval and consent to participate

The studies were approved and consented to by Ruijin Hospital Ethics Committee. The patients provided their written informed consent to participate in this research. The ethics committee reference number is (2019) □□□□ (158)□.

Consent for publication

Not applicable.

Competing interests

The authors declare that they have no competing interests

References

1. Strobel O, Neoptolemos J, Jager D, Buchler MW: **Optimizing the outcomes of pancreatic cancer surgery**. Nat Rev Clin Oncol 2019, **16**(1):11–26.
2. Siegel RL, Miller KD, Jemal A: **Cancer statistics, 2020**. CA Cancer J Clin 2020, **70**(1):7–30.
3. Hong F, Gong Z, Zhang X, Ma P, Yin Y, Wang H: **Identification of biomarkers and ceRNA network in glioblastoma through bioinformatic analysis and evaluation of potential prognostic values**. Ann Transl Med 2021, **9**(20):1561.

4. Xiao S, Liu X, Yuan L, Wang F: **A Ferroptosis-Related lncRNAs Signature Predicts Prognosis and Therapeutic Response of Gastric Cancer**. Front Cell Dev Biol 2021, **9**:736682.
5. Wei G, Dong Y, He Z, Qiu H, Wu Y, Chen Y: **Identification of hub genes and construction of an mRNA-miRNA-lncRNA network of gastric carcinoma using integrated bioinformatics analysis**. PLoS One 2021, **16**(12):e0261728.
6. Diboun I, Wernisch L, Orengo CA, Koltzenburg M: **Microarray analysis after RNA amplification can detect pronounced differences in gene expression using limma**. BMC Genomics 2006, **7**:252.
7. Agarwal V, Bell GW, Nam JW, Bartel DP: **Predicting effective microRNA target sites in mammalian mRNAs**. Elife 2015, **4**.
8. Chen Y, Wang X: **miRDB: an online database for prediction of functional microRNA targets**. Nucleic Acids Res 2020, **48**(D1):D127-D131.
9. Paraskevopoulou MD, Vlachos IS, Karagkouni D, Georgakilas G, Kanellos I, Vergoulis T, Zagganas K, Tsanakas P, Floros E, Dalamagas T *et al*: **DIANA-LncBase v2: indexing microRNA targets on non-coding transcripts**. Nucleic Acids Res 2016, **44**(D1):D231-238.
10. Liao Y, Wang J, Jaehnig EJ, Shi Z, Zhang B: **WebGestalt 2019: gene set analysis toolkit with revamped UIs and APIs**. Nucleic Acids Res 2019, **47**(W1):W199-W205.
11. Tang Z, Li C, Kang B, Gao G, Li C, Zhang Z: **GEPIA: a web server for cancer and normal gene expression profiling and interactive analyses**. Nucleic Acids Res 2017, **45**(W1):W98-W102.
12. Tomczak K, Czerwinska P, Wiznerowicz M: **The Cancer Genome Atlas (TCGA): an immeasurable source of knowledge**. Contemp Oncol (Pozn) 2015, **19**(1A):A68-77.
13. Consortium GT: **The Genotype-Tissue Expression (GTEx) project**. Nat Genet 2013, **45**(6):580–585.
14. Vasaikar S, Straub P, Wang J, Zhang B: **LinkedOmics: Analyzing multi-omics data within and across 32 cancer types**. Cancer Research 2019, **79**(13).
15. Huang S, Xue P, Han X, Zhang C, Yang L, Liu L, Wang X, Li H, Fu J, Zhou Y: **Exosomal miR-130b-3p targets SIK1 to inhibit medulloblastoma tumorigenesis**. Cell Death Dis 2020, **11**(6):408.
16. Mu HQ, He YH, Wang SB, Yang S, Wang YJ, Nan CJ, Bao YF, Xie QP, Chen YH: **MiR-130b/TNF-alpha/NF-kappaB/VEGFA loop inhibits prostate cancer angiogenesis**. Clin Transl Oncol 2020, **22**(1):111–121.
17. Du L, Liu W, Aldana-Masangkay G, Pozhitkov A, Pichiorri F, Chen Y, Rosen ST: **SUMOylation inhibition enhances dexamethasone sensitivity in multiple myeloma**. J Exp Clin Cancer Res 2022, **41**(1):8.
18. Ou C, Peng NF, Li H, Peng YC, Li LQ: **The potential mechanism of miR-130b on promotion of the invasion and metastasis of hepatocellular carcinoma by inhibiting Notch-Dll1**. J Recept Signal Transduct Res 2020, **40**(2):157–165.
19. Yan W, Wang Y, Chen Y, Guo Y, Li Q, Wei X: **Exosomal miR-130b-3p Promotes Progression and Tubular Formation Through Targeting PTEN in Oral Squamous Cell Carcinoma**. Front Cell Dev Biol 2021, **9**:616306.
20. Liu J, Zhou R, Deng M, Xue N, Li T, Guo Y, Gao L, Fan R, Zhao D: **Long non-coding RNA DIO3OS binds to microRNA-130b to restore radiosensitivity in esophageal squamous cell carcinoma by upregulating PAX9**. Cancer Gene Ther 2021.
21. Gu JJ, Fan KC, Zhang JH, Chen HJ, Wang SS: **Suppression of microRNA-130b inhibits glioma cell proliferation and invasion, and induces apoptosis by PTEN/AKT signaling**. Int J Mol Med 2018, **41**(1):284–292.

22. Ge W, Goga A, He Y, Silva PN, Hirt CK, Herrmanns K, Guccini I, Godbersen S, Schwank G, Stoffel M: **miR-802 Suppresses Acinar-to-Ductal Reprogramming During Early Pancreatitis and Pancreatic Carcinogenesis**. Gastroenterology 2022, **162**(1):269–284.
23. Tijunelyte I, Malbec R, Chami B, Cacheux J, Dez C, Leichle T, Cordelier P, Bancaud A: **micro-RNA 21 detection with a limit of 2 pM in 1 min using a size-accordable concentration module operated by electrohydrodynamic actuation**. Biosens Bioelectron 2021, **178**:112992.
24. Wang X, Yu H, Sun W, Kong J, Zhang L, Tang J, Wang J, Xu E, Lai M, Zhang H: **The long non-coding RNA CYTOR drives colorectal cancer progression by interacting with NCL and Sam68**. Mol Cancer 2018, **17**(1):110.
25. Chen T, Zhu C, Ye C: **LncRNA CYTOR attenuates sepsis-induced myocardial injury via regulating miR-24/XIAP**. Cell Biochem Funct 2020.
26. Galamb O, Kalmar A, Sebestyen A, Danko T, Kriston C, Furi I, Hollosi P, Csabai I, Wichmann B, Krenacs T *et al*: **Promoter Hypomethylation and Increased Expression of the Long Non-coding RNA LINC00152 Support Colorectal Carcinogenesis**. Pathol Oncol Res 2020.
27. Liu Y, Li M, Yu H, Piao H: **lncRNA CYTOR promotes tamoxifen resistance in breast cancer cells via sponging miR125a5p**. *Int J Mol Med* 2020, **45**(2):497–509.
28. Chen W, Du M, Hu X, Ma H, Zhang E, Wang T, Yin L, He X, Hu Z: **Long noncoding RNA cytoskeleton regulator RNA promotes cell invasion and metastasis by titrating miR-613 to regulate ANXA2 in nasopharyngeal carcinoma**. Cancer Med 2020, **9**(3):1209–1219.
29. Zheng X, Dong S, Sun L, Xu J, Liu J, Hao R: **LncRNA LINC00152 Promotes Laryngeal Cancer Progression by Sponging MiR-613**. Open Med (Wars) 2020, **15**:240–248.
30. Zhang J, Li W: **Long noncoding RNA CYTOR sponges miR-195 to modulate proliferation, migration, invasion and radiosensitivity in nonsmall cell lung cancer cells**. Biosci Rep 2018, **38**(6).
31. Yue B, Liu C, Sun H, Liu M, Song C, Cui R, Qiu S, Zhong M: **A Positive Feed-Forward Loop between LncRNA-CYTOR and Wnt/beta-Catenin Signaling Promotes Metastasis of Colon Cancer**. Mol Ther 2018, **26**(5):1287–1298.
32. Cheng Y, Xiong HY, Li YM, Zuo HR, Liu Y, Liao GL: **LncRNA HOXA11-AS promotes cell growth by sponging miR-24-3p to regulate JPT1 in prostate cancer**. Eur Rev Med Pharmacol Sci 2021, **25**(14):4668–4677.
33. Xia H, Niu Q, Ding Y, Zhang Z, Yuan J, Jin W: **Long noncoding HOXA11-AS knockdown suppresses the progression of non-small cell lung cancer by regulating miR-3619-5p/SALL4 axis**. J Mol Histol 2021, **52**(4):729–740.
34. Padam KSR, Basavarajappa DS, Shenoy US, Chakrabarty S, Kabekkodu SP, Hunter KD, Radhakrishnan R: **In silico interaction of HOX cluster-embedded microRNAs and long non-coding RNAs in oral cancer**. J Oral Pathol Med 2022, **51**(1):18–29.
35. Xu Y, Ren Z, Wang X, Ren M: **The lncRNA HOXA11-AS acts as a tumor promoter in breast cancer through regulation of the miR-125a-5p/TMPRSS4 axis**. J Gene Med 2022:e3413.
36. You L, Wu Q, Xin Z, Zhong H, Zhou J, Jiao L, Song X, Ying B: **The long non-coding RNA HOXA11-AS activates ITGB3 expression to promote the migration and invasion of gastric cancer by sponging miR-124-3p**. Cancer Cell Int 2021, **21**(1):576.

37. Li XL, Wang B, Yang FB, Chen LG, You J: **HOXA11-AS aggravates microglia-induced neuroinflammation after traumatic brain injury**. Neural Regen Res 2022, **17**(5):1096–1105.

Figures

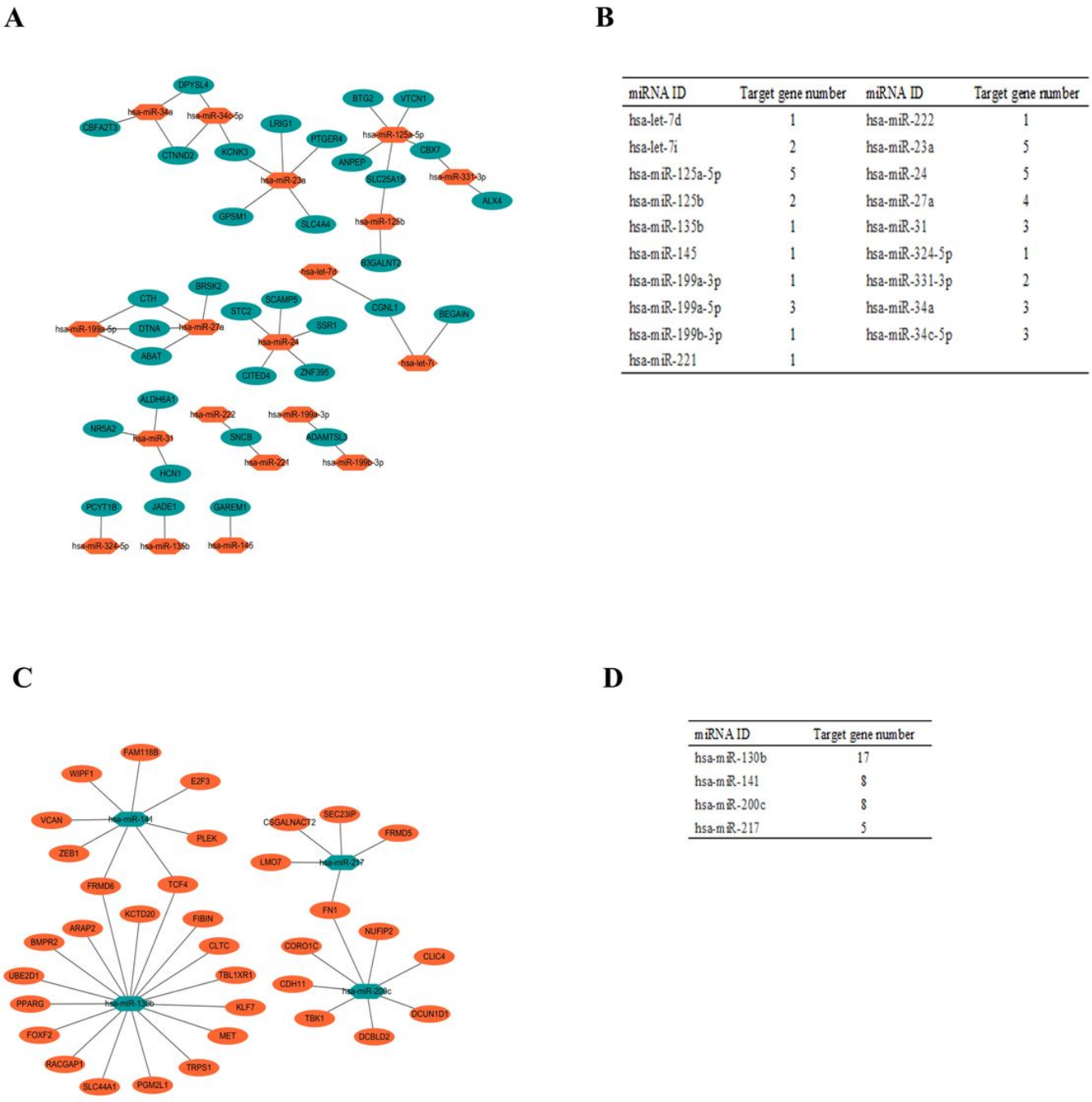

miRNA ID	Target gene number	miRNA ID	Target gene number
hsa-let-7d	1	hsa-miR-222	1
hsa-let-7i	2	hsa-miR-23a	5
hsa-miR-125a-5p	5	hsa-miR-24	5
hsa-miR-125b	2	hsa-miR-27a	4
hsa-miR-135b	1	hsa-miR-31	3
hsa-miR-145	1	hsa-miR-324-5p	1
hsa-miR-199a-3p	1	hsa-miR-331-3p	2
hsa-miR-199a-5p	3	hsa-miR-34a	3
hsa-miR-199b-3p	1	hsa-miR-34c-5p	3
hsa-miR-221	1		

miRNA ID	Target gene number
hsa-miR-130b	17
hsa-miR-141	8
hsa-miR-200c	8
hsa-miR-217	5

Figure 1

Potential target genes of DE-miRNAs predicted by miRWalk. (A) Upregulated DEmiRNAs-target genes network; (B) Target gene count for corresponding upregulated DEmiRNA; (C) Downregulated DEmiRNAs-target genes network;

(D) Target gene count for corresponding downregulated DEmiRNAs.

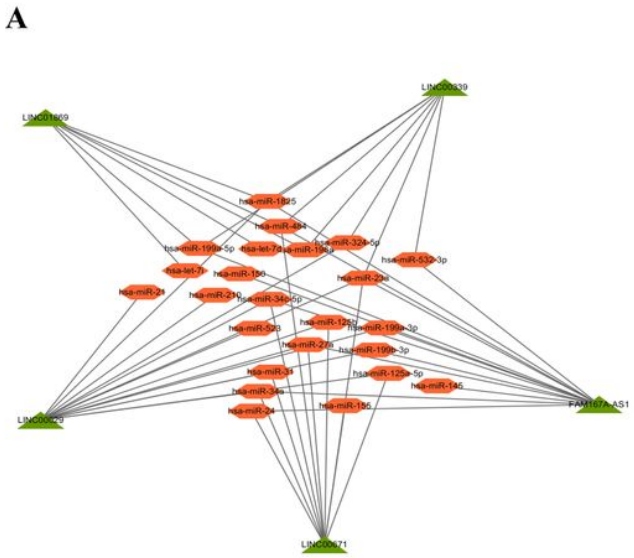

B

miRNA ID	Target lncRNA number	miRNA ID	Target lncRNA number
hsa-let-7d	1	hsa-miR-210	1
hsa-let-7i	1	hsa-miR-23a	2
hsa-miR-125a-5p	2	hsa-miR-23a	4
hsa-miR-125b	2	hsa-miR-24	2
hsa-miR-145	1	hsa-miR-27a	3
hsa-miR-150	1	hsa-miR-31	2
hsa-miR-155	1	hsa-miR-324-5p	2
hsa-miR-1825	4	hsa-miR-34a	3
hsa-miR-196a	2	hsa-miR-34c-5p	3
hsa-miR-199a-3p	2	hsa-miR-484	4
hsa-miR-199a-5p	3	hsa-miR-523	1
hsa-miR-199b-3p	2	hsa-miR-532-3p	2
hsa-miR-21	1		

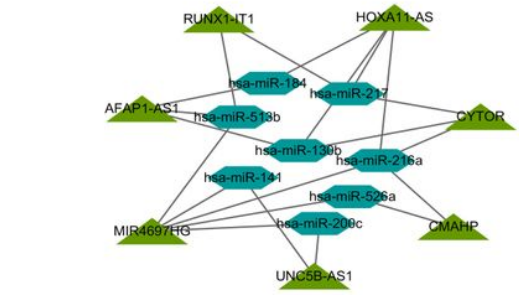

D

miRNA ID	Target lncRNA number
hsa- miR-141	2
hsa- miR-184	2
hsa- miR-217	3
hsa- miR-130b	3
hsa- miR-200c	2
hsa- miR-216a	4
hsa-miR-513b	3
hsa-miR-526a	2

Figure 2

DElncRNAs-DEmiRNAs pairs predicted by LncBase. (A) Upregulated DEmiRNAs-DElncRNAs genes network; (B) Target DElncRNAs count for each upregulated DEmiRNAs; (C) Downregulated DEmiRNAs- DElncRNAs network; (D) Target DElncRNAs count for each downregulated DEmiRNAs.

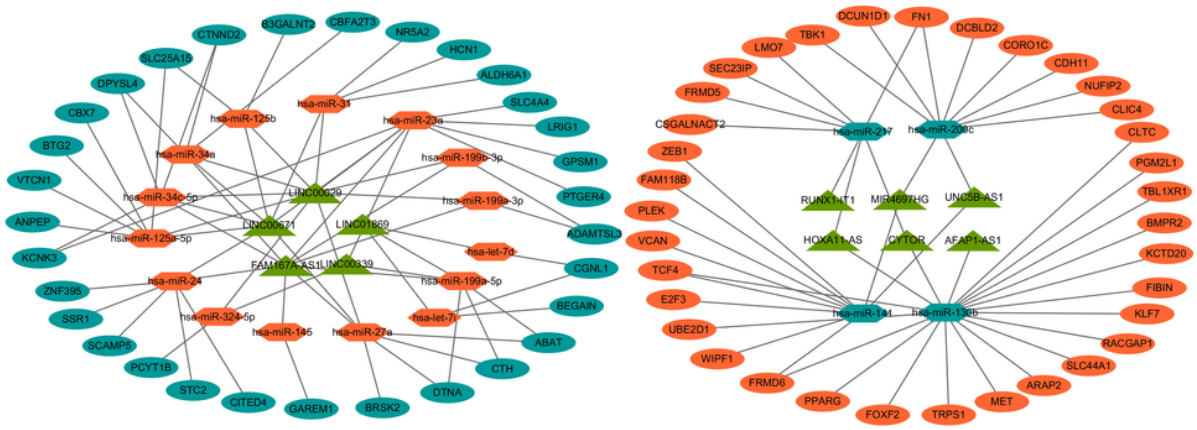

Figure 3

lncRNA-miRNA-mRNA regulatory network. There were 11 DElncRNAs, 19 DEmiRNAs, 66 DEmRNAs and 121 edges in the network.

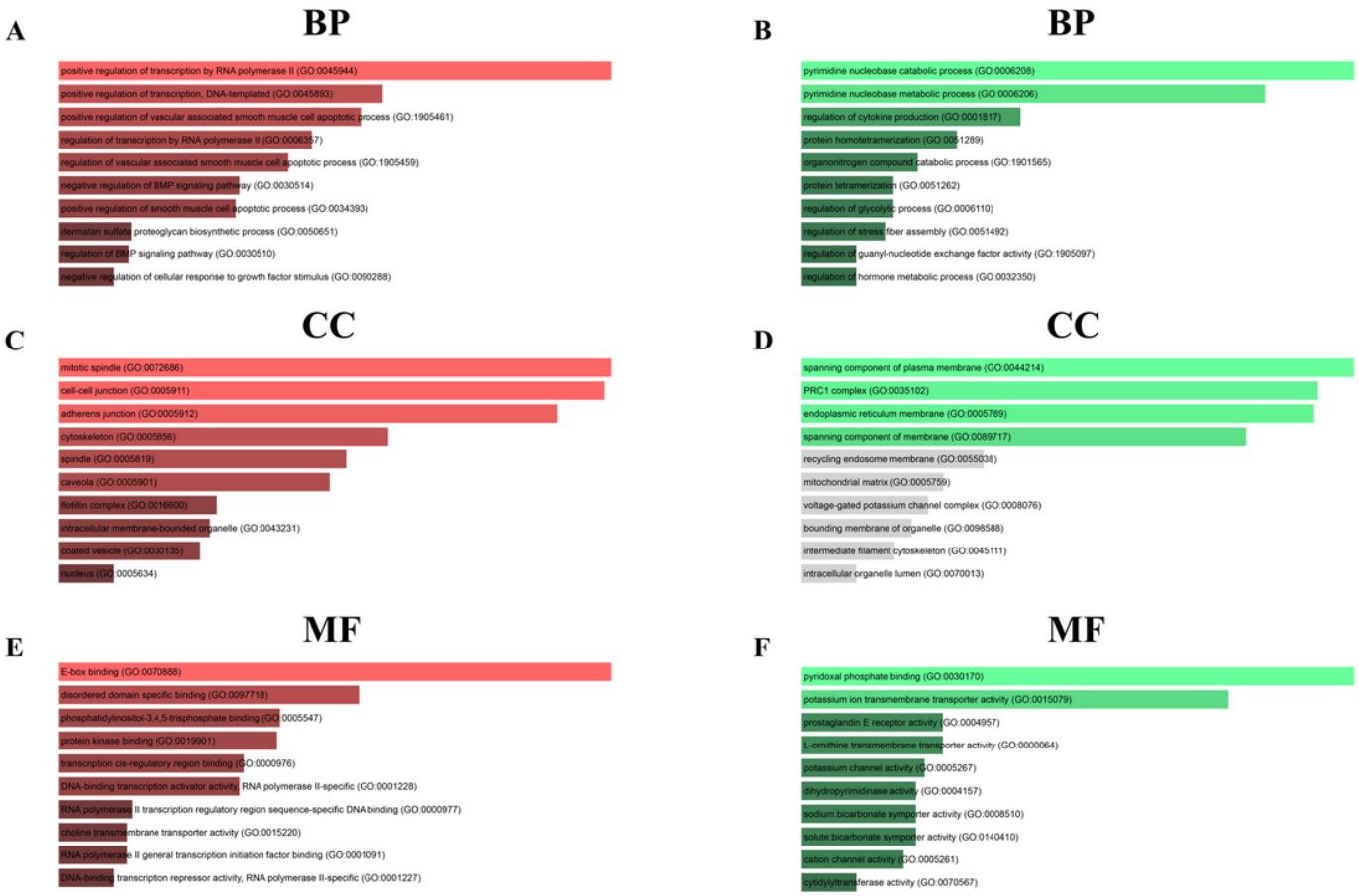

Figure 4

GO enrichment analysis of candidate genes. The top 10 BP (A), CC (C), and MF (F) items in upregulated candidate genes; The top 10 BP (B), CC (D), and MF (E) items in downregulated candidate genes.

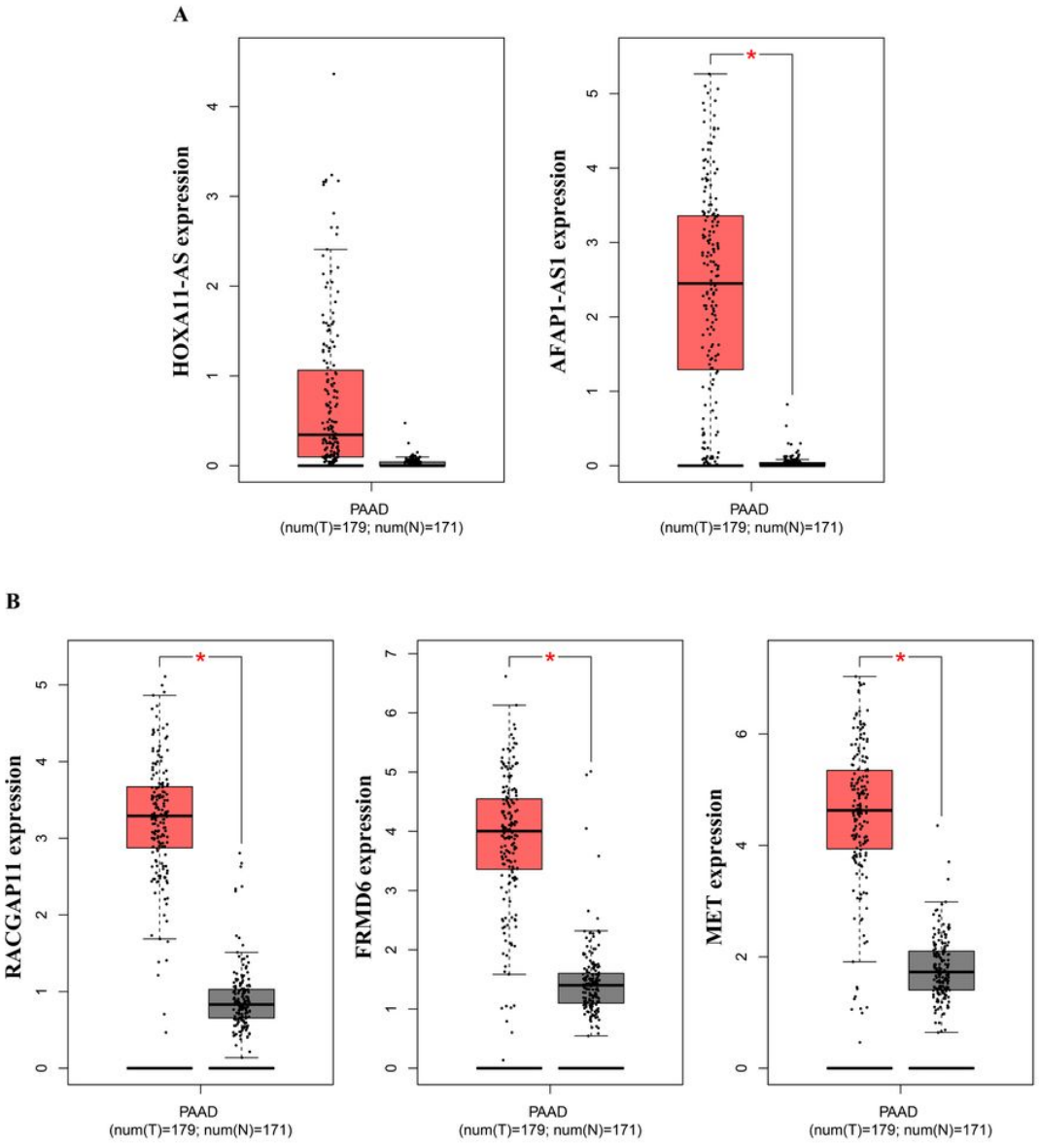

Figure 5

Expression analysis of DElncRNAs(A) and DEmRNAs(B) by GEPIA. The red boxes represent the gene expression in pancreatic cancer tissues (n=179), the grey boxes represent the gene expression in normal pancreas tissues (n=171).

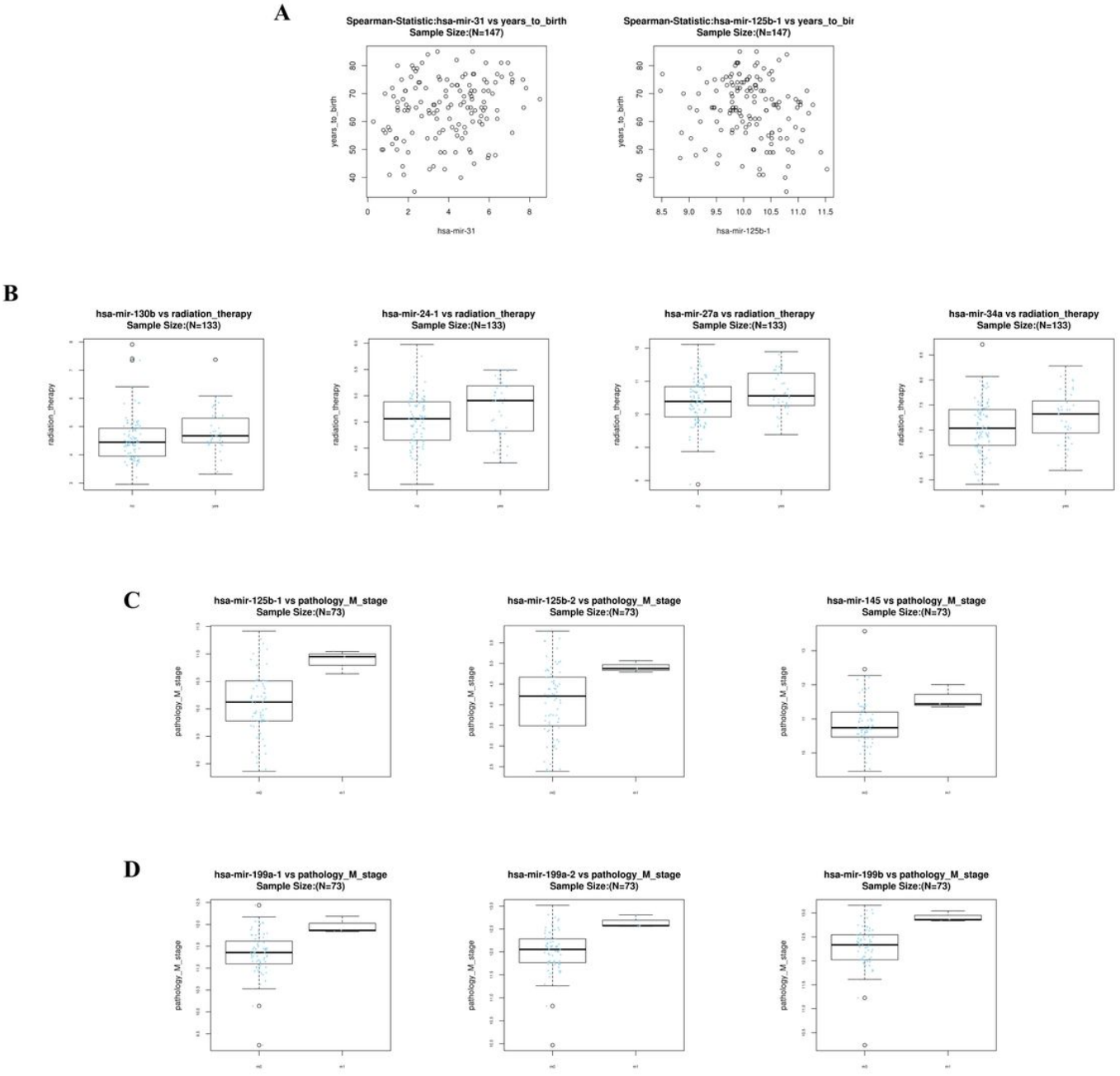

Figure 6

The correlation between DEmiRNAs contained in the ceRNA network and years to birth (A), radiation therapy (B), pathology M stage(C-D).

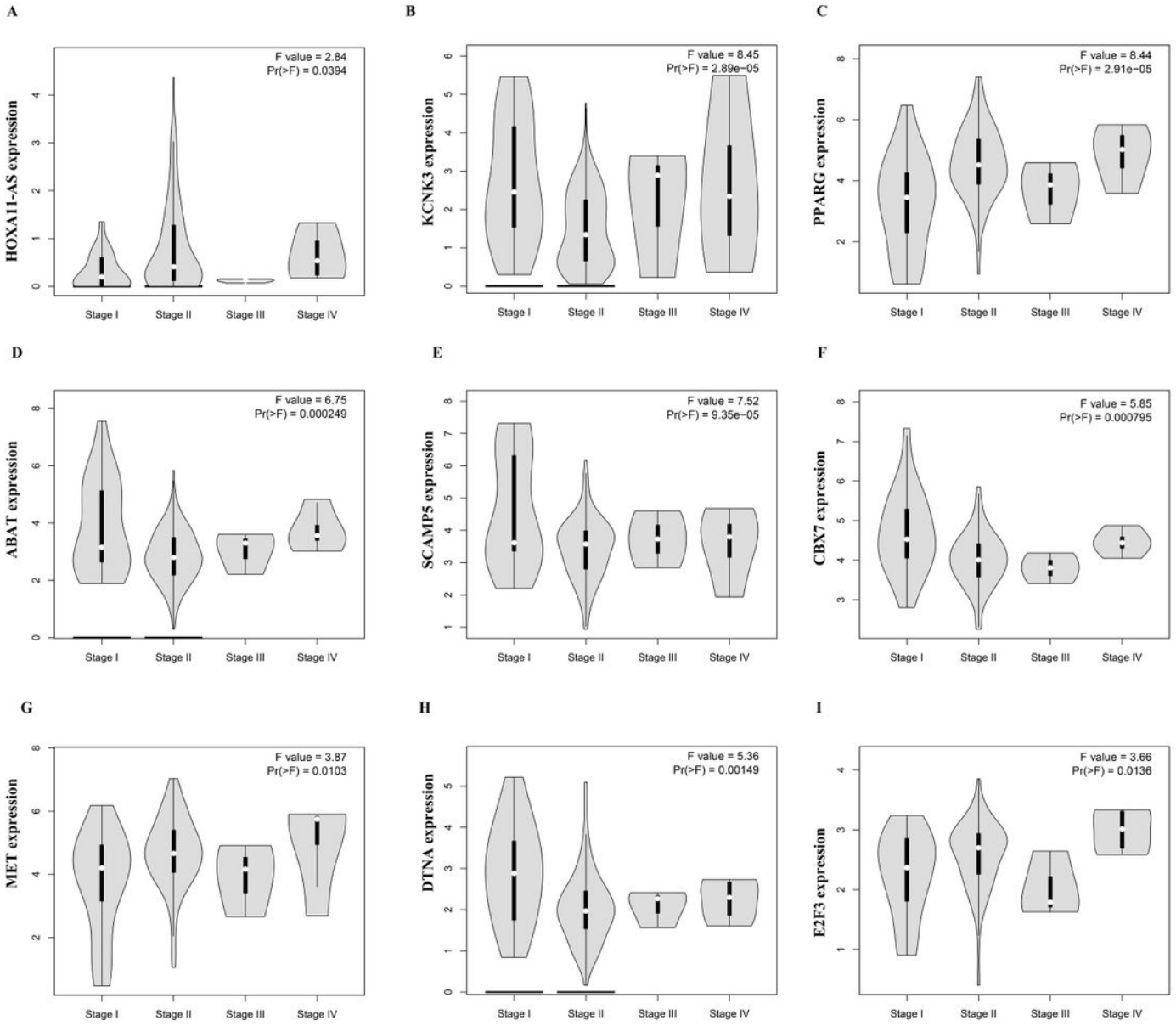

Figure 7

The significant correlation between 1 DElncRNAs (A), top 8 DEmRNAs (B-I) involved in the ceRNA regulatory network and pathologic stage.

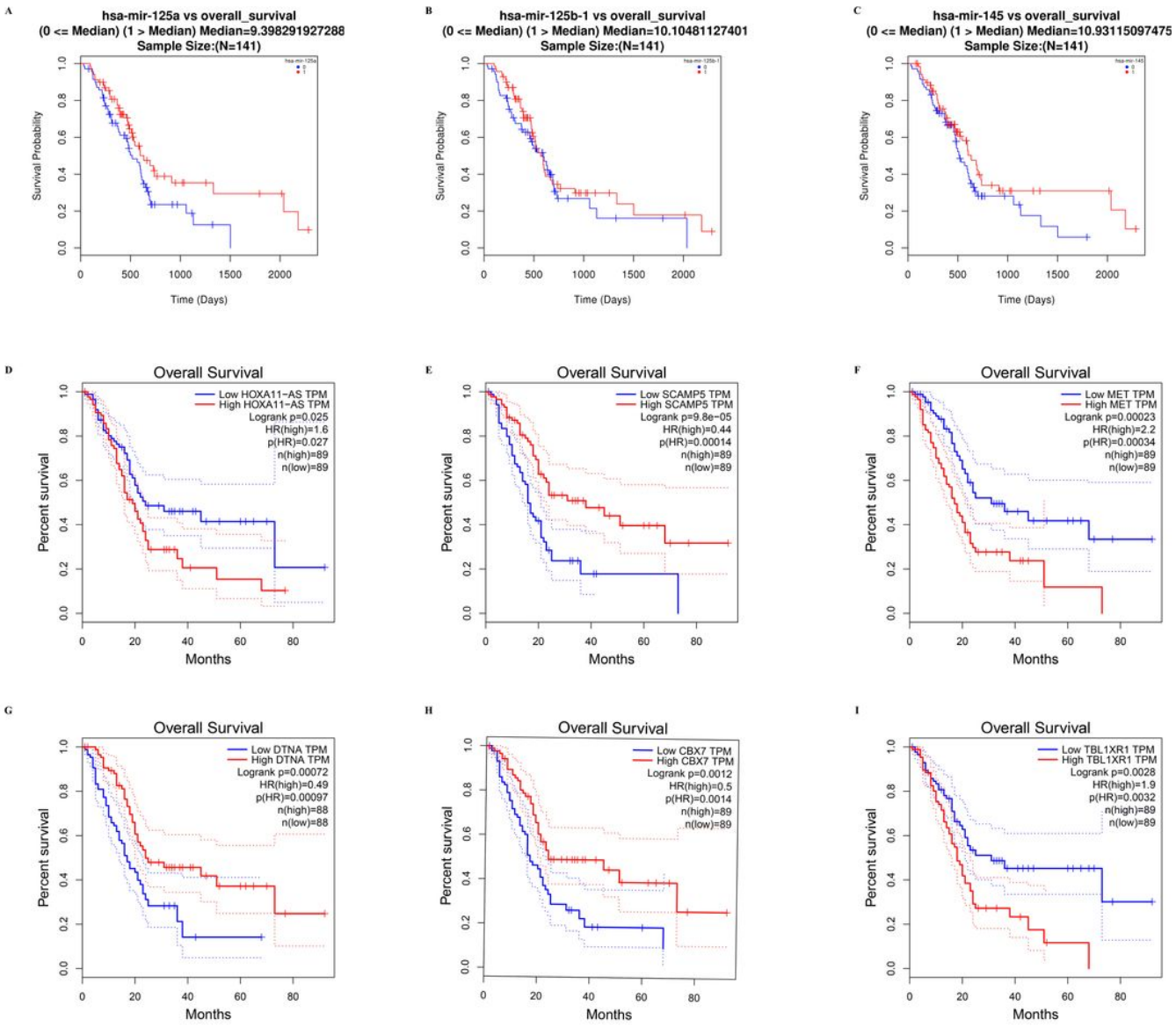

Figure 8

Overall survival curves for the 3 miRNAs(A-C), 1 lncRNA(D) and top 5 DEmRNAs(E-I), based on the best cutoff for pancreatic cancer in TCGA

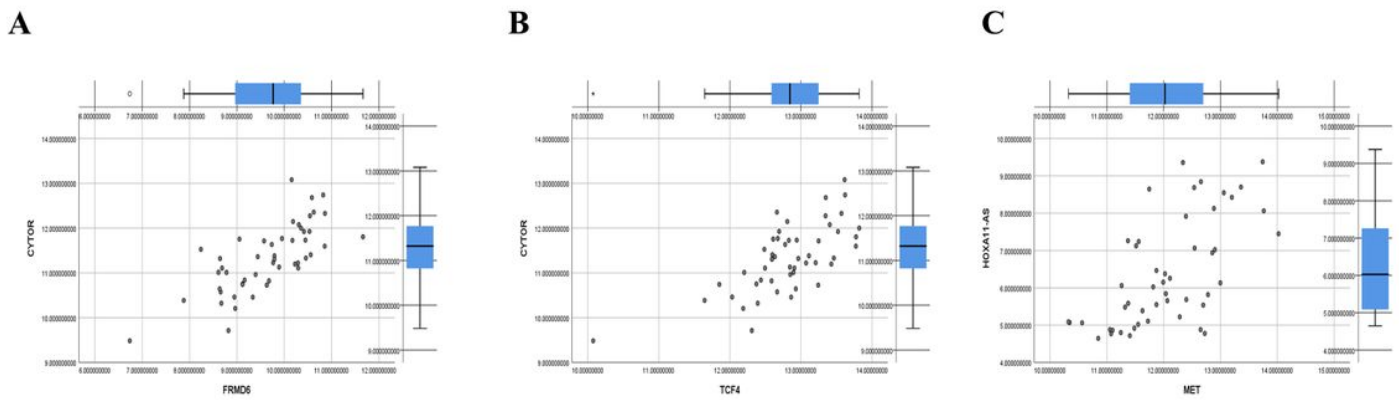

Figure 9

Regression analysis between DElncRNAs and DEmRNAs expression targeted by hsa-miR-130b in the ceRNA regulatory network (the top 3 correlation coefficients are shown).

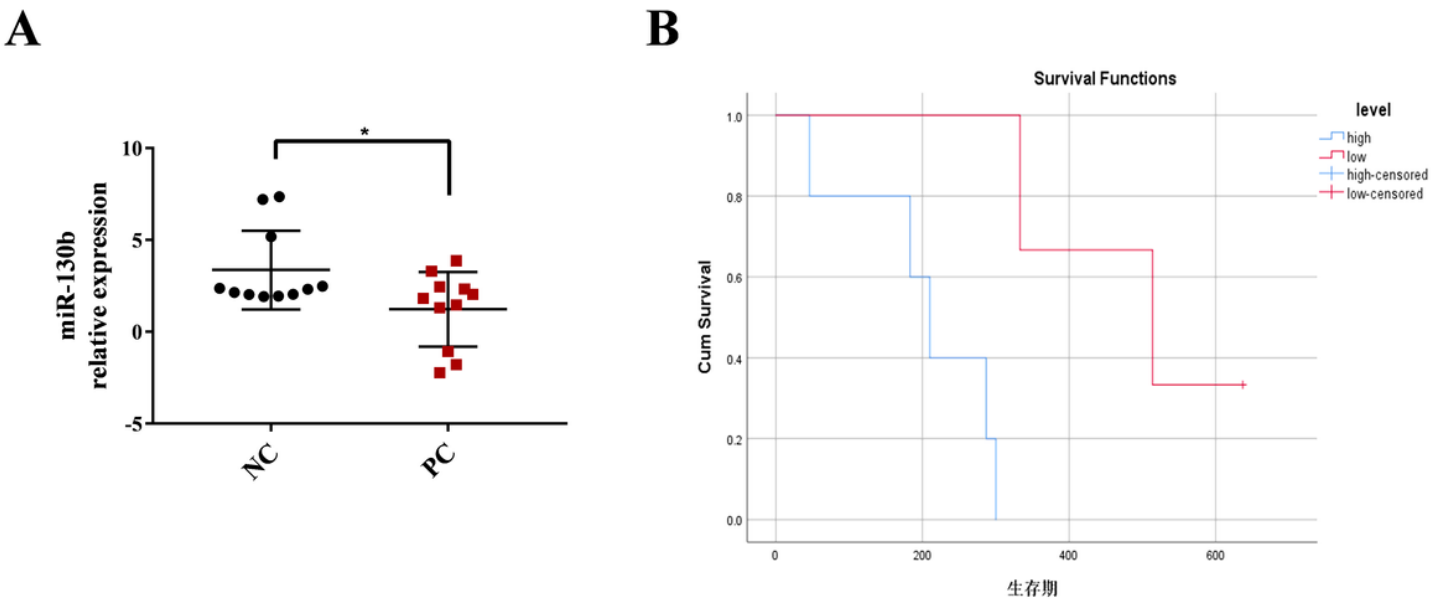

Figure 10

Analysis of miR-130b expression level in PC tissues and the survival. (A) The relative expression of miR-130b in PC tissues (n=11) and paired NC tissues (n=11). (B) Kaplan-Meier curves of the overall survivals time of 11 PC patients in downregulated expression level (below median, n=5) and upregulated expression (above median, n=6) according to the miR-130b expression. The low-expression of miR-130b was strongly associated with a poor overall survival time.

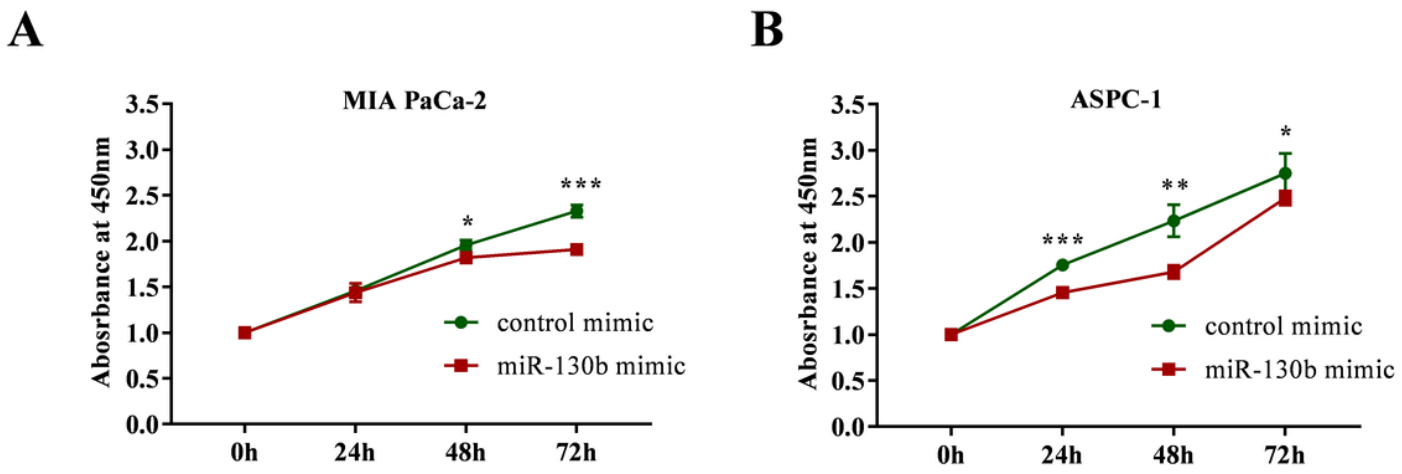

Figure 11

Overexpression of miR-130b resulted in increasing PC cell proliferation. A) CCK-8 assay in MIA PaCa-2 cells 6h after transfection with mimic and control B) CCK-8 assay in ASPC-1 cells 6h after transfection with mimic and control. All experiments were performed in 5 replicates and t tests (unpaired) were used to evaluate results

Figure 12

miR-130b overexpression facilitated PC cell migration ability. (A) After transfection with control or mimic for 24 h, linear wounds were generated in ASPC-1 cells and monitored every 24 h. (B) After transfection with control or inhibitor for 24 h, linear wounds were generated in ASPC-1 cells and monitored every 24 h. (C) After transfection with control or mimic for 24 h, linear wounds were generated in MIA PaCa-2 cells and monitored every 24 h. (D) After transfection with control or inhibitor for 24 h, linear wounds were generated in MIA PaCa-2 cells and monitored every 24 h. Three replications were performed for each experiment

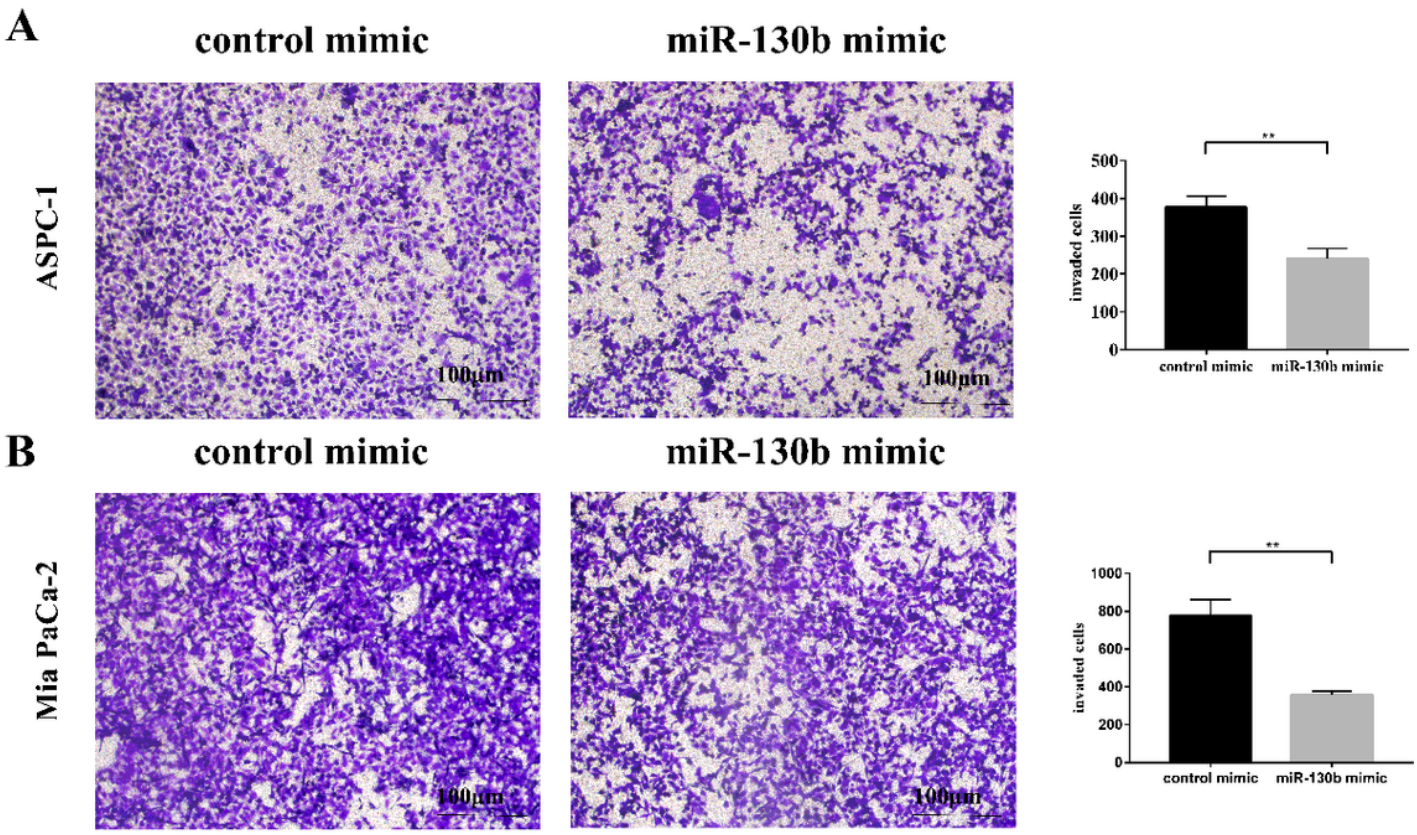

Figure 13

MiR-130b inhibited the migration of pancreatic cancer cells. (A) The ASPC-1 cells were transfected with miR-130b mimic and control mimic (50 nM) for 48 hours. (B) The MIA PaCa-2 cells were treated as above. **. P<0.01 as significance.

Supplementary Files

This is a list of supplementary files associated with this preprint. Click to download.

- supplementarymaterial.docx